Langmuir

Article

pubs.acs.org/Langmuir

What Is the Contact Angle of Water on Graphene?

Fereshte Taherian, Valentina Marcon, and Nico F. A. van der Vegt*

Center of Smart Interfaces, Technische Universität Darmstadt, Petersenstrasse 17, D-64287, Darmstadt, Germany

Frédéric Leroy*

Eduard-Zintl-Institut für Anorganische und Physikalische Chemie, Technische Universität Darmstadt, Petersenstrasse 22, D-64287, Darmstadt, Germany

ABSTRACT: Although experimental and theoretical studies have addressed the question of the wetting properties of graphene, the actual value of the contact angle of water on an isolated graphene monolayer remains unknown. While recent experimental literature indicates that the contact angle of water on graphite is in the range 90−95°, it has been suggested that the contact angle on graphene may either be as high as 127° or moderately enhanced in comparison with graphite. With the support of classical molecular dynamics simulations using empirical force-fields, we develop an argumentation to show that the value of 127° is an unrealistic estimate and that a value of the order of 95−100° should be expected. Our study establishes a connection between the variation of the work of adhesion of water on graphene-based surfaces and the interaction potential between individual water molecules and these surfaces. We show that a variation of the contact angle from 90° on graphite to 127° on graphene would imply that both of the first two carbon layers of graphite contribute approximately the same interaction energy with water. Such a situation is incompatible with the short-range nature of the interaction between water and this substrate. We also show that the interaction potential energy between water and the graphene-based substrates is the main contribution to the work of adhesion of water with a relative magnitude that is independent of the number of graphene layers. We introduce the idea that the remaining contribution is entropic in nature and is connected to the fluctuations in the water−substrate interaction energy.

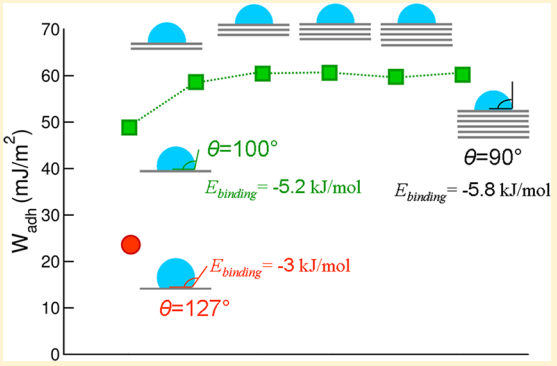

1. INTRODUCTION

Since its discovery, graphene has attracted a great deal of attention both in academia and in industry due to its exceptional properties. Graphene is expected to find applications in numerous domains of nanotechnology as varied as optoelectronics[1] and water desalination[2] among others. The dispersion of graphene flakes in polymers[3] or the interaction of graphene sheets with aqueous solutions of salts strongly depends on the wetting properties of graphene. Graphene has already been recognized as a hydrophobic material. However, quantitative knowledge of its wetting properties is still missing. Therefore, the precise characterization of these properties is of crucial importance and became a topic of investigation recently. We call graphene the two-dimensional planar material made up of a monolayer of carbon atoms in contrast to other authors who use the term graphene to describe materials composed of a few carbon layers.

A simple way to address the wetting properties of graphene with respect to water is to measure the contact angle of a water droplet deposited on an isolated graphene surface. Measuring a contact angle in this precise case depends on the possibility to isolate and to suspend monolayers of carbon atoms. Moreover, the dimensions of such samples should be sufficiently extended to support liquid droplets that are large enough so that they do not evaporate too fast. The material should be free of roughness as this factor may significantly influence the results of the measurements. Although obtaining such experimental conditions may be a challenge, several experimental works have addressed the question of the wetting properties of graphene. It was shown that there is no thickness dependence of the contact angle of water from measurements on single, bi-, and multilayer graphene coated on SiC.[4] This finding was generalized, and it was shown that water had a different contact angle on a single graphene layer depending on the type of supporting substrate.[5,6] In the recent study of Wang et al.,[7] graphene monolayers or a stack of a very few graphene layers were produced through chemical exfoliation of natural graphite flakes. The contact angle of water was measured on several such flakes. The influence of the supporting substrate was removed by stacking several flakes on top of each other. Under these conditions, it was found that water had a contact angle of 98.3° on graphite, while this quantity increased to 127° on graphene. Such a high value would promote graphene to be the most hydrophobic smooth material. Indeed, the most direct

Received: November 21, 2012
Revised: January 12, 2013
Published: January 15, 2013

   dx.doi.org/10.1021/la304645w | *Langmuir* 2013, 29, 1457−1465

competitor would be crystalline *n*-perfluoroeicosane, which yields a contact angle of water of 119°.[8] However, the measurements of the contact angle reported above were done on a film composed of several graphene flakes. These experimental conditions may have led to a sample exhibiting significant ruggedness and thus may explain the origin of the high value of the contact angle.[4] Scocchi et al.[9] recently formulated the idea that those measurements may be seen as the most reliable characterization of the contact angle of water on graphene in the ideal condition of a flat surface free of defects. These authors developed a new empirical force field for the water−carbon interaction on the basis of the contact angle of 127°. On the basis of the experimental works of Wang et al.,[7] Shin et al.,[4] and Rafiee et al.[5] performed between 2009 and 2012, we note that a value of approximately 90−95° seems to be an acceptable estimate of the contact angle of water on graphite. The question we address in the present work is whether a value of the contact angle on a monolayer of graphene of the order of 127° is compatible with a value of the contact angle of approximately 90−95° on graphite. Shih et al.[6] have very recently contributed to this issue by developing a theory according to which the contact angle of water on monolayer graphene is 96°.

Besides recent achievements in the experimental approach to the characterization of the wetting properties of graphene, quantum-based simulation methods recently made significant progresses. Indeed, recent advances in electronic density functional theory, which account for the van der Waals interactions in the interaction energies, made it possible to better describe the interactions between single water molecules or small water clusters and solid surfaces such as graphite or graphene (see ref 10 and references therein). Quantum molecular dynamics (QMD) simulations were recently employed to study a water droplet on graphene. A value of the contact angle of 87° was obtained.[11] It must be noted that the droplet employed in these computations contained only 125 water molecules. This small number suggests that the result may strongly be affected by the line tension, that is, an important size effect that has been characterized both in experiments[12] and in molecular simulations.[13−15] Moreover, the stability of such small droplets may be questioned from the standpoint of experiments,[16] although submicrometer-sized droplets have recently been observed at the step-edges of graphene surfaces.[17] Nevertheless, it must be noted that the value obtained in the QMD study mentioned above is close to the range of values commonly accepted for the contact angle of water on graphite, that is, around 90°. Despite the uncertainty that characterizes that result, it strongly contrasts with the experimental value of 127° in the experimental work mentioned previously.

In this Article, we show that the value of 127° for the contact angle of water on graphene is an overestimation of the actual value. To that end, we develop a theoretical argumentation based on interfacial thermodynamics. The development of this model is supported by classical molecular dynamics (MD) simulations. We reproduce the result previously obtained both analytically and by molecular simulations, which shows that the contact angle of a water droplet on graphite is insensitive to the number of carbon atoms layers as long as this number is larger than or equal to three.[5,6,18] We show that a value of 127° for the contact angle of water on graphene is obtained by means of an interaction potential between water and graphene that is incompatible with the accepted value of the contact angle of approximately 90° on graphite. Our work delivers important information about the wetting properties of graphene and leads to multiple conclusions. Besides the importance of the information about contact angles on graphene in the context of experimental materials science, the precise knowledge of such a macroscopic property is required to generate reliable interaction potentials that are employed in molecular simulations. Such a topic is illustrated in the reviews by Werder et al.[13] and by Alexiadis and Kassinos[19] in the context of the molecular modeling of the interactions between water and carbon based materials. From a more fundamental point of view, the theoretical approach we develop shows that the work of adhesion of water on graphite or graphene is mainly due to the interaction energy between water and these surfaces. On the basis of the theory of solvation, we introduce the idea that the remaining part is entropic in nature and finds its origin in the fluctuations of the water−substrate interaction energy. This contribution is overlooked in the theories based on the approach of Hamaker, which is employed in the work of Rafiee et al.[5] and Shih et al.,[6] for example.

To reach our conclusions, we develop a model to connect the variations of the work of adhesion on graphene-based substrates to the change in the interaction potential between water and these substrates. We employ MD simulations to probe the assumptions we formulate. Our argumentation requires that interfacial tensions, contact angles, potential interaction energies, and interaction potentials of a single water molecule with the surfaces are computed. In section 2, we describe the systems we studied and provide technical details on how these quantities were obtained. The results of the related calculations and the derivation of the model are presented and discussed in section 3 before the conclusions of our work are summarized in the last section. The reader mostly interested in the results of this study may read section 2.1 before directly reading section 3.

2. METHODOLOGY

2.1. Free Energy Calculations. We computed the interfacial tension between water and graphite. To that end, we employed the thermodynamic integration-based phantom-wall algorithm implemented in a modified version of the MD package YASP.[20] Although this algorithm has been described in detail elsewhere,[20,21] we recall its main features because it is one of the key elements of the derivation of our thermodynamic model. Our computations were carried out using periodic boundary conditions in all directions of space. Therefore, graphite was modeled as a slab, and water was present on both sides of it (see ref 20 for details about the implementation). According to the phantom-wall algorithm, graphite was reversibly turned into a flat repulsive surface. This transformation was realized by the action of two walls (the phantom walls), which became the repulsive surfaces mentioned above at the end of the process. The walls were initially present within the graphite slab but were far enough from water not to interact with it. They were progressively symmetrically displaced in the direction perpendicular to the interface. Thus, the interaction with the water molecules was progressively established while graphite was insensitive to them. This interaction yielded water to be lifted off from the graphite substrate. At the end of the process, the walls were displaced far enough from their initial positions so that water only interacted with them and no longer with graphite. The free energy change of the process is the work required to lift off water from graphite by the action of the walls. Note that this process was conducted at constant cross-sectional area of the solid substrate, constant pressure, constant temperature, and constant number of particles. Consequently, the Gibbs free energy change per unit of cross-sectional area is also the difference in interfacial tension between the initial and final systems. Note that a pressure × volume term has to

be taken into account to include the possible volume change of the system in connection with the transformation mentioned above.[20] To describe the interactions between water and the repulsive walls, we employed a planar Weeks−Chandler−Andersen (WCA) potential,[22] which is dependent on the water−wall distance. In this case, it was shown by Chandler and co-workers[23,24] that the related interfacial tension is the surface tension of water γ_{lv}. Indeed, water tends to avoid the repulsive surface by forming a thin liquid−vapor interface in its vicinity. Therefore, the interfacial tension that describes such an interface is γ_{lv}. In summary, we computed the difference in interfacial tension $\Delta\gamma$ between a water-repulsive surface interface characterized by the interfacial tension γ_{lv} and the water−graphite interface characterized by the interfacial tension γ_{sl}. We also independently determined γ_{lv} by means of the so-called mechanical route.[25] Thus, γ_{sl} was finally obtained through $\gamma_{sl} = \gamma_{lv} - \Delta\gamma$. Such computations have already been carried out by one of the present authors in the context of carbon-based materials with the exception that poorly attractive phantom walls were employed.[26]

The SPC/E model of water was used[27] in combination with the interaction potential of Werder et al. between water and graphite.[13] According to this model, the water−carbon interaction is modeled by means of a 12-6 Lennard-Jones potential between the carbon and the oxygen atoms. The distance and energy parameters are $\sigma = 0.319$ nm and $\varepsilon = 0.392$ kJ/mol, respectively. These values warrant that the contact angle of droplets free of the effect of the line tension reproduces the macroscopic experimental value of 86° against which the intermolecular interactions were optimized.[13] No electrostatic interaction is taken into account between water and graphite. The internal dynamics of graphite was modeled through the potential of Bedrov and Smith.[28] The cross-sectional area of the system was 4.26 × 3.69 nm^2. The graphite slab contained seven stacked graphene sheets, although water only interacted with the first two top such layers on each side of the slab due to the value of the interaction cutoff. The system contained 4158 molecules of water. The electrostatic interactions were treated by means of the reaction field method with an infinite reaction field dielectric constant. The cutoff distance for the water−water interactions was 1.5 nm, while it was 1.0 nm for the carbon−water interactions and carbon−carbon interactions. The thermostat and barostat of Berendsen et al.[27] were used to maintain temperature and pressure at 298 K (with a coupling constant of 0.2 ps) and 101.3 kPa (with a coupling constant of 2.0 ps), respectively. The computations consisted of equilibration runs of 250 ps followed by production runs of 500 ps. Data were extracted every 1 ps for further statistical analysis.

2.2. Contact Angle Calculations. The study of the contact angles of water droplets containing 4000 molecules was carried out with GROMACS.[29] We performed simulations with graphene-based systems in which the number of graphene monolayers n in the sample was varied between $n = 1$−6. In these simulations, the carbon atoms were fixed at the crystallographic positions of the graphite lattice with a carbon−carbon distance of 0.142 nm and an interlayer distance of 0.34 nm. The SPC/E model of water was employed to describe water−water interactions. The electrostatic interactions were computed by means of the particle mesh Ewald (PME) technique.[30] The model of Jaffe et al.[18] was employed for the water−carbon interactions. In this model, the interactions are described identically to the model of Werder et al.[13] mentioned in the free energy calculations with the exception that a cutoff distance of 2.0 nm is employed. Consequently, the Lennard-Jones distance and energy parameters are $\sigma_{CO} = 0.319$ nm and $\varepsilon_{CO} = 0.357$ kJ/mol so as to reproduce the value of the macroscopic contact angle of water on graphite too. Note that the models of Werder et al.[13] and the model of Jaffe et al.[18] yield identical results as far as the structure of water in the vicinity of graphite is concerned. To model the graphene system with a macroscopic contact angle of 127° (noted $n = 1^*$ in what follows), we used a procedure similar to the one recently developed by Scocchi et al.[9] to obtain the values of the Lennard-Jones parameters between the oxygen and carbon atoms. In accord with this study, we found values of $\sigma_{CO} = 0.319$ nm and $\varepsilon_{CO} = 0.205$ kJ/mol. This force-field was used in combination with a cutoff of 2.0 nm. The computations were performed in the canonical ensemble by means of the Nosé−Hoover thermostat with a coupling constant of 0.2 ps.

It must be noted that we performed simulations with droplets of which the size yields a deviation from the macroscopic contact angle. Because of the effect of line tension, the contact angle of the droplets that include 4000 water molecules on graphite has a value of 90.2 ± 0.3° in our computations, whereas the value of 86° is obtained for larger droplets free of line tension. The values of the surface tension of water in the reaction field and the PME simulations agree within the uncertainty. At 298 K, the reaction-field treatment yields a value of 59.1 ± 1.3 mJ/m^2, whereas the PME computations lead to a value of 60.3 ± 1.8 mJ/m^2.

2.3. Interaction Energies and Potentials Calculations. Films having a thickness of approximately 6 nm and containing 8000 water molecules were employed to compute the time averaged total potential interaction energy $u_{ws,n}$ of water with the systems $n = 1$−6 and $n = 1^*$ previously defined. The cross-sectional area of the systems was 6.396 × 6.389 nm^2. $u_{ws,n}$ was obtained following:

$$u_{ws,n} = \frac{1}{N_t}\sum_{i=1}^{N_t}\left(\sum_{j=1}^{N_{C,n}}\sum_{k=1}^{N_O} v_{jk}(r)\right) \quad (1)$$

In eq 1, N_t refers to the number of independent configurations used to calculate the average, $N_{C,n}$ is the number of carbon atoms in the system with n carbon layers, and N_O is the number of oxygen atoms (i.e., water molecules) in the films. v_{jk} is the interatomic interaction potential between the carbon and oxygen atoms at a distance r apart. The configurations of the system employed to compute $u_{ws,n}$ were obtained by means of MD simulations with GROMACS in the canonical ensemble similarly to the contact angle calculations. To that end, simulations of 10 ns were used, and 5000 configurations separated by 2 ps were extracted.

We also computed the average interaction potentials V between single water molecules and the surfaces $n = 1$−6 and $n = 1^*$ by means of

$$V_n(z) = \frac{1}{D}\iint_D \sum_{j=1}^{N_{C,n}} v_j(x, y, z)\,dx\,dy \quad (2)$$

Note that V only depends on the height z of the water molecules above the planar surfaces $n = 1$−6 and $n = 1^*$. In practice, the continuous summation in eq 2 is performed by discretizing the xy plane parallel to the carbon surfaces into surface elements having an area of 0.05 × 0.05 nm^2. A single water molecule is placed on a lattice point at a given z distance above the surface. The total interaction energy between the water molecule and graphite is computed over the domain of integration D. D is determined by the interaction cutoff used in the contact angle calculations. This operation is repeated until water has been placed on each lattice point of the unit cell of graphite. The average value of the interaction potential energies in eq 2 leads to V at the given height z.

3. RESULTS AND DISCUSSION

3.1. Enthalpy and Entropy of the Work of Adhesion. To show that a value of 127° of the contact angle θ of water on a graphene monolayer is inconsistent with a value of 90° on graphite, we derive a relationship between the work of adhesion W_a of water on the surfaces $n = 1$−6 and $n = 1^*$ and the interaction potential V between water and these surfaces. We start with Young's equation according to which the equilibrium contact angle θ of a macroscopic droplet placed on a flat solid substrate can be described by:[31]

$$\gamma_{lv}\cos\theta = \gamma_{sv} - \gamma_{sl} \quad (3)$$

where γ_{lv}, γ_{sv}, and γ_{sl} are the liquid−vapor, solid−vapor, and the solid−liquid interfacial tensions, respectively. Although θ and γ_{lv} can be obtained by independent measurements, this is not

dx.doi.org/10.1021/la304645w | Langmuir 2013, 29, 1457−1465

the case for γ_{sv} and γ_{sl}.[32] Therefore, only the difference $\gamma_{sv} - \gamma_{sl}$ is directly accessible from experiments. In the case of low vapor density fluids like water and poorly wettable substrates like graphene and graphite, we assume that the contribution of γ_{sv} to the contact angle is much lower than γ_{sl}. In fact, this assumption has already been quantitatively verified by molecular simulations in the case of water on graphite.[26,33] It can also be noted that Werder et al.[13] showed by means of MD simulations that both flexible and rigid models of graphite yield the same contact angle of water in addition to the fact that γ_{sv} exactly cancels out in the limit of rigid substrates.[34] Under that condition, eq 3 yields:

$$\Delta\gamma = \gamma_{lv} - \gamma_{sl} = \gamma_{lv}(1 + \cos\theta) \quad (4)$$

Equation 4 can be interpreted as the result of a phantom-wall calculation as mentioned in section 2.1. Indeed, $\Delta\gamma$ is the difference in interfacial tension between a system characterized by γ_{lv} where water interacts with a purely repulsive substrate and a system with the interfacial tension γ_{sl} where water interacts with a carbon-based solid surface. The fact that the interfacial tension of the repulsive interface is γ_{lv} and that γ_{sv} is a negligible quantity yields $\Delta\gamma$ to be the work of adhesion $W_a = \gamma_{lv}(1 + \cos\theta)$ of water on the graphene-based substrates. Furthermore, the quantity $A\Delta\gamma = A(\gamma_{lv} - \gamma_{sl})$ is the difference in the excess interfacial Gibbs free energy when a surface like graphite or graphene is turned into a repulsive surface. It is equal to the Gibbs free energy change of the transformation provided that the number of water molecules and the number of particles in the substrate remain constant, and that the transformation is performed at constant temperature, constant cross-sectional area, and constant pressure normal to the interfaces. The Gibbs free energy change $A\Delta\gamma$ can be written as the sum of an enthalpy contribution and an entropy contribution: $A\Delta\gamma = \Delta H - T\Delta S$. According to eq 4, there is a relationship between $\Delta\gamma$ and cos θ. Consequently, the computation of ΔH and ΔS and the study of the temperature dependence of $\Delta\gamma$ may be compared to possible experimental determinations of cos θ at different temperatures. This is particularly important to address the reliability of the computations of $\Delta\gamma$. The temperature dependence of $A\Delta\gamma$ was obtained by means of MD through phantom-wall computations in the case of water on graphite in the temperature range 283–328 K. It is shown in Figure 1 that there is a linear relationship between $\Delta\gamma$ and temperature in the range that was sampled. We fitted a linear equation to the simulation data and found $\Delta S/A = 0.140 \pm 0.017$ mJ/m^2·K and $\Delta H/A = 103.7 \pm 5.1$ mJ/m^2. The value of $\Delta\gamma$ at each temperature has been reported in Table 1.

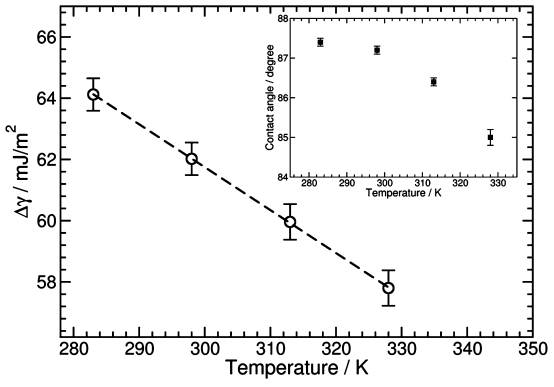

Figure 1. Temperature variations of $\Delta\gamma$. The "○" are the simulation results. The dashed line represents a linear regression to the simulations. Inset: Temperature variation of water contact angle on graphite as predicted by the MD simulations.

Table 1. Interfacial Tension and Contact Angle Values of Water on Graphite Depending on Temperature

temp (K)	$\Delta\gamma$ (mJ/m^2)	γ_{lv}	γ_{sl}	θ
283	64.1 ± 0.5	61.3 ± 1.3	−2.8 ± 1.8	87.4 ± 0.1
298	62.0 ± 0.5	59.1 ± 1.3	−2.9 ± 1.8	87.2 ± 0.1
313	60.0 ± 0.6	56.4 ± 1.3	−3.6 ± 1.9	86.4 ± 0.1
328	57.8 ± 0.6	53.2 ± 1.3	−4.6 ± 1.9	85.0 ± 0.2

ΔS is the change in entropy between the repulsive surface system and the graphite system. It is interesting to note that ΔS has a positive value. To understand the physical meaning of this result, we reported in Figure 2 the mass–density distribution of water in the direction perpendicular to the surface of graphite (black curve). This plot was obtained from the analysis of our MD simulations. Two relatively intense maxima can be observed on the plot. This is interpreted as water forming two layers on graphite, as was already obtained in previous studies.[13,26] In contrast, the interface with the purely repulsive substrate features no layering of water (see the dashed line in Figure 2). This is actually a consequence of water preserving its hydrogen-bonding network by forming a thin liquid–vapor interface in the vicinity of the repulsive hydrophobic surface as was mentioned in section 2.1. We can conclude that the configurations of water close to graphite are more constrained than those close to the repulsive surface. This result explains why entropy is gained ($\Delta S > 0$) when water is moved from the structured interface on graphite to the virtually unconstrained interface on the repulsive substrate. We will comment in detail the origin of the positive sign of ΔH later in the text.

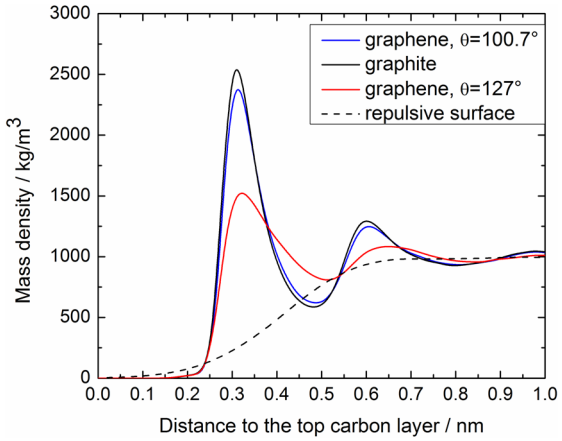

Figure 2. Water mass–density distribution as a function of the distance to the top layer of carbon atoms of graphite and graphene. Black curve: Water–graphite. Blue curve: Water–graphene with θ = 100.7°. Red curve: Water–graphene with θ = 127°. Dashed curve: Water in contact with the repulsive surface.

One may wonder whether the values of ΔS and ΔH obtained in the simulations are in any manner comparable to experiments. This raises the question as to whether the model employed in the computations is able to capture the temperature dependence of the contact angle of water on graphite. Despite the apparent simplicity of the system at hand,

dx.doi.org/10.1021/la304645w | Langmuir 2013, 29, 1457–1465

Table 2. Thermodynamic Data for the Water Graphite and Water Graphene Systems[a]

	θ	$\gamma_{lv}(1 + \cos\theta)$ (mJ/m^2)	$\Delta H_{ws}/A$ (mJ/m^2)	$T\Delta S_{ws}/\Delta H_{ws}$	$W_{a,n}/W_{a,n=6}$	$\Delta H_{ws,n}/\Delta H_{ws,n=6}$	E_b (kJ/mol)
n = 1	100.7 ± 0.4	49.1 ± 2.2	76.9	0.36 ± 0.02	0.82 ± 0.01	0.85	−5.22
n = 2	91.3 ± 0.3	58.9 ± 1.9	87.9	0.33 ± 0.01	0.98 ± 0.01	0.97	−5.70
n = 3	89.7 ± 0.3	60.6 ± 1.8	90.1	0.33 ± 0.01	1.01 ± 0.01	0.99	−5.78
n = 4	89.6 ± 0.2	60.7 ± 1.7	90.7	0.33 ± 0.01	1.01 ± 0.01	1.00	−5.80
n = 5	90.4 ± 0.3	59.9 ± 1.8	90.8	0.34 ± 0.01	1.00 ± 0.01	1.00	−5.81
n = 6	90.2 ± 0.3	60.1 ± 1.8	90.7	0.34 ± 0.01	1	1	−5.81
n = 1*	127.0 ± 0.3	24.0 ± 2.7	35.8	0.33 ± 0.03	0.40 ± 0.01	0.39	−3.00

[a]The uncertainty on $\Delta H_{ws}/A$ is of the order of 0.1% and was omitted.

no conclusive experiments have been reported yet. Osborne recently discussed the difficulties encountered in such an experimental study.[35] In fact, the measurements are very sensitive to the experimental conditions, and it is even difficult to discriminate between both of the situations where θ may increase or decrease with temperature. In this context, the test of the validity of the values of ΔS and ΔH relies on theoretical and simulation works that aim to make up for the momentary lack of experimental results. Garcia et al.[36] recently predicted by means of a theoretical analytical approach based on the sharp-kink approximation that the contact angle of water on graphite should decrease with temperature.[36] This trend is in line with the work carried out by Choong[33] by means of the Monte Carlo simulations scheme developed by Errington and successive co-workers[37] and the work of Dutta et al.[38] performed by means of MD simulations. However, these studies show that the temperature dependence of the contact angle is relatively weak below the boiling point of water. We employed our results for γ_{lv} and γ_{sl} in Table 1 to compute the temperature dependence of θ in the range 283−328 K by means of eq 4 in which we neglected γ_{sv} as stated above. The result is shown in the inset of Figure 1. The trend we obtained is consistent with the studies of Garcia et al.,[36] Dutta et al.,[38] and Choong.[33] To be more quantitative, we extracted the value of ΔS and ΔH per unit area from the interfacial tensions in the work of Choong at 300K and 350 K and assumed linear dependence of $\Delta\gamma$ on temperature. The values we obtained are in agreement with our own result for $\Delta S/A$ (0.137 and 0.140 ± 0.017 mJ/m^2·K, respectively) and $\Delta H/A$ (99.2 and 103.7 ± 5.1 mJ/m^2, respectively). On the basis of those comparisons, we are confident that our study follows the trends outlined in the earlier theoretical and simulation studies that predict that the contact angle of water on graphite is a decreasing function of temperature.

3.2. Work of Adhesion and Interaction Potentials. Before we proceed further with our argumentation, we should mention that the MD simulations to which we will refer in what follows deal with water droplets on graphite and different models of graphene systems as detailed in section 2.2. We performed simulations of water droplets on the surfaces n = 1 to n = 6 and calculated the respective contact angles. The results are reported in Table 2 and plotted in Figure 3. It can be seen that the contact angle on graphite converges at n = 3. A comparable behavior was recently reported both experimentally and in MD simulations.[5] It can also be observed that a value of the contact angle of 100.7° is observed on the n = 1 surface (i.e., graphene) without modification of the intermolecular interaction between water and the carbon atoms. This observation contrasts with the value of 127° and is in line with the idea that the contact angle on graphite and graphene

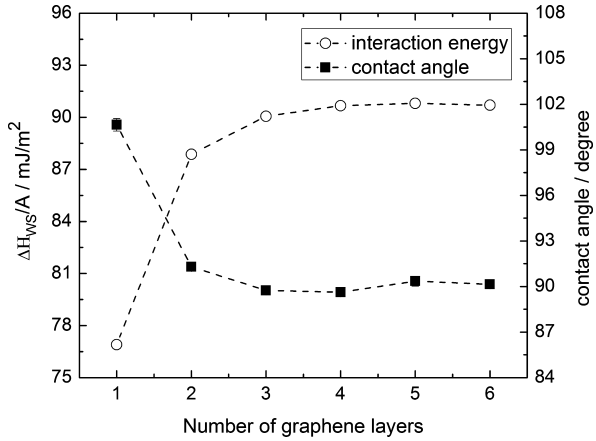

Figure 3. Water−substrate potential interaction energy with respect to the number of carbon layers in the substrate (○). Contact angle variation with respect to the number of carbon layers in the substrate (■). The dashed line is a guide to the eye. The error bars are smaller than the symbols.

may only differ by a few degrees as was also noted by Shih et al.[6]

We note that the change in enthalpy ΔH defined above arises from two contributions. On the one hand, when graphite or graphene are turned into the purely repulsive surface, there is a change in the interactions between water and the actual substrate. We call ΔH_{ws} this contribution to ΔH. On the other hand, the change in the water structure in the vicinity of graphite or graphene (as is illustrated in Figure 2) and the repulsive substrate yields a change in the water−water interactions. Indeed, it can be observed in Figure 2 that graphite (n = 6) and both models of graphene (n = 1 and n = 1*) yield water to form layers (black, blue ,and red curves, respectively), although the intensity of the first maximum in water mass density is lower in the case of n = 1* (θ = 127°) than in the case of n = 1 (θ = 100.7°). The effect of the change in the water structure between the carbon surfaces and the repulsive interface on the change in enthalpy is quantified by a contribution ΔH_{ww}. The enthalpy change ΔH is the sum of two contributions, $\Delta H = \Delta H_{ws} + \Delta H_{ww}$. Note that there is no change in ΔH arising from the interactions within the solid because these interactions remain unchanged in the phantom-wall calculations (see section 2.1). To compute the enthalpy changes, we use the relationship $\Delta H = \Delta U + P\Delta V$, where U is the internal energy, P is the pressure, and V is the volume. The water layering in the vicinity of the surfaces yields the change in PV per unit area to be of the order of 0.1 mJ/m^2 101.3 kPa, which is negligible when compared to the energies featured previously. Therefore, the change in enthalpy was obtained assuming that $\Delta H \approx \Delta U$. Moreover, because the systems have

dx.doi.org/10.1021/la304645w | Langmuir 2013, 29, 1457−1465

the same number of particles, there is no change in the total kinetic energy and $\Delta U = \Delta u$, where u is the total interaction potential energy. In our computations, the interatomic interaction potentials are based on Lennard-Jones and Coulomb pair interactions. Therefore, u can be written as a sum of three contributions $u = u_{ww} + u_{ws} + u_{ss}$. u_{ws} is the total interaction potential energy arising from the water−substrate interactions, whereas u_{ww} is the total interaction potential energy arising from the water−water interactions and u_{ss} is the total potential interaction energy within the solid. Thus, we obtain the relationships $\Delta H_{ws} = \Delta u_{ws}$ and $\Delta H_{ww} = \Delta u_{ww}$, which show that the enthalpy changes can be directly obtained from the changes in the interaction potential energies. Note that $\Delta u_{ss} = 0$ for the reason that there is no change of interactions within the substrate. Combining $\Delta H = \Delta H_{ws} + \Delta H_{ww}$ and $A\Delta\gamma = \Delta H - T\Delta S$ with eq 4 yields:

$$W_a = \gamma_{lv}(1 + \cos\theta) = \frac{1}{A}(\Delta H_{ws} + \Delta H_{ww} - T\Delta S) \quad (5)$$

Note that eq 5 arises from the equality between the work of adhesion and the free energy change $\Delta\gamma$ of turning a carbon-based surface into a repulsive wall. $\Delta\gamma$ can be interpreted as the difference in solvation free energy per unit area between two such surfaces. It was shown in the framework of the theory of solvation that the contribution of the solvent−solvent interaction to the free energy of solvation is strictly enthalpy−entropy compensating.[39,40] In other words, there is no contribution of these interactions to the solvation free energy. This result yields the enthalpy term ΔH_{ww} in eq 5 to be exactly compensated by an entropy term in $-T\Delta S$. Thus, $\Delta H_{ww} - T\Delta S$ simplifies to $-T\Delta S_{ws}$, where ΔS_{ws} is the entropy change in connection with the interaction between water and both the carbon-based substrates and the repulsive surface. Equation 5 takes the following form:

$$W_a = \frac{1}{A}(\Delta H_{ws} - T\Delta S_{ws}) \quad (6)$$

Another result of the solvation theory is that the entropy contribution to the free energy of solvation arises from the fluctuations in the solute−solvent interactions.[41,42] Therefore, the work of adhesion can be understood as arising from the water−substrate interaction strength ($\Delta H_{ws}/A$) and the fluctuations of these interactions ($-T\Delta S_{ws}/A$). This interpretation is in line with the work of Garde and co-workers[43] who showed that the fluctuations in water density in the vicinity of solid substrates play a key role in determining the hydrophilic/hydrophobic nature of substrates. We computed the value of ΔH_{ws} in eq 6 as the total water−substrate interaction potential energy $-u_{ws}$ by means of MD simulations for all of the values of n (see section 2.3). It must be recalled that water tends to minimize the interaction with the repulsive surface. Consequently, we observed that the potential interaction energy between water and the repulsive substrates is several orders of magnitude smaller than in the case of the carbon-based surfaces and could be neglected. We plotted in Figure 3 the variations of $\Delta H_{ws}/A$ (i.e., $-u_{ws,n}/A$) as a function of the number of carbon layers. It can be observed that this quantity is independent of the number of layers if $n > 2$. Such a behavior was also observed for the contact angle (Figure 3). We assumed that the relationship in eq 5 holds true for all of the systems studied here. The values of γ_{lv}, θ, and $\Delta H_{ws}/A$ were employed to obtain $-T\Delta S_{ws}$. It can be seen in Table 2 that the quantity $T\Delta S_{ws}$ represents approximately 33% of ΔH_{ws} in all cases. Note that this result was obtained using the value of γ_{lv} of the model employed in our computations (60.3 mJ/m^2). Values of approximately 17% are obtained if the experimental value of γ_{lv} (72 mJ/m^2) is considered. This observation suggests that $\Delta H_{ws}/A$ is the main contribution to the work of adhesion W_a. However, the entropy contribution must be taken into account to obtain a quantitative description, as mentioned above. The roughly constant ratio between $T\Delta S_{ws}$ and ΔH_{ws} leads to the following relationship:

$$\frac{W_{a,n}}{W_{a,n=6}} \approx \frac{\Delta H_{ws,n}}{\Delta H_{ws,n=6}} \quad (7)$$

It can be observed in Table 2 that very good agreement exists between both the independent determinations of the ratio between the works of adhesion and the right-hand side of eq 7. Equation 7 shows that there is a direct relationship between the change in the work of adhesion and the change in the water substrate interaction potential energy. $\Delta H_{ws}/A$ can also be defined following:

$$\frac{\Delta H_{ws}}{A} = \int_0^\infty V(z)\rho(z)\,dz \quad (8)$$

where $V(z)$ is the total interaction potential between a given surface and a water molecule located at a distance z from this surface (see section 2.3) and $\rho(z)$ is the water number-density distribution perpendicular to the surface. We have reported in Figure 4 the computed variations of $V(z)$ for water interacting with graphite and graphene (both for $\theta = 100.7°$ and 127°). We quantitatively verified that these variations could be described by the following analytical form $V(z) = 4\pi\varepsilon d(\sigma^{12}/5z^{10} - \sigma^6/2z^4)$,[44] where σ and ε are the Lennard-Jones distance and energy parameters of the nonbonded interactions between the carbon atoms and the water molecules, while d is the surface density of carbon atoms in a graphene sheet ($d = 38.1$ nm^{-2}). It can be noted that that analytical form is short-ranged when compared to the form derived from the approach of Hamaker for other materials such as metals where the dispersion part of the potential is proportional to $1/z^3$.[45] In the case of graphite ($n = 6$), the variations of V can be fitted to $V(z) = A/z^{10} - B/z^4 - C/z^3$, where the $1/z^3$ term takes into account the carbon layers

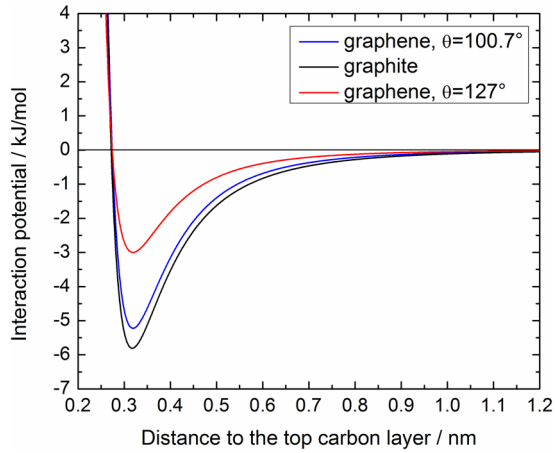

Figure 4. Potential interaction energy for a single water molecule in interaction with graphite and graphene as a function of the distance to the surface. Black curve: Graphene ($\theta = 100.7°$). Red curve: Graphite. Blue curve: Graphene ($\theta = 127°$).

dx.doi.org/10.1021/la304645w | Langmuir 2013, 29, 1457−1465

that are added to the top layer in agreement with the Steele potential.[46]

Recent quantum calculations reported results for the equilibrium distance and binding or adsorption energy of water molecules on graphene and graphite.[10,47] These computations were performed with a single water molecule and therefore do not include the collective effects that arise from a computation including several molecules. In single molecule calculations, the most stable configuration for water is obtained when the two bonds are oriented toward the carbon surfaces.[10] Such a configuration may not be realistic in a system including several water molecules as it would imply that two hydrogen bonds per water molecule are sacrificed. Instead, it was shown that water tends to minimize the number of such sacrificed hydrogen bonds in the vicinity of graphite[26] and other substrates that do not form hydrogen bonds with water. The empirical force-fields used in our classical MD simulations implicitly include such many-particles effects because the water−carbon Lennard-Jones interaction parameters were optimized to reproduce the contact angles of water, that is, a collective property. Nevertheless, the single molecule quantum computations yield a good indication of how equilibrium distances and binding/adsorption energies of water vary between graphite and graphene. The interaction potential V related to the intermolecular interactions in our MD simulations has an equilibrium distance of 0.319 nm for graphene (both for θ = 100.7° and 127°) and 0.3175 nm for graphite (see Figure 4). These values compare well with recent single molecule quantum calculations (0.32−0.34 nm).[10,47] The minimum of the interaction potential V is the binding energy E_b of water on the related surface. We reported in Table 2 this energy for the systems n = 1−6 and n = 1*. In the case of graphite, quantum calculations studies led to average values of the binding energy of −13.1[10] and −15 kJ/mol,[47] while average values of −10.4[10] and −13.3 kJ/mol[47] were obtained for graphene. These values are overestimates of the results obtained by means of empirical force-fields. This observation may be explained by the fact that these results were obtained by means of computations carried out on a single water molecule, as noted above. Here again, precise experimental data are lacking to perform a complete comparison.

It can be noted that the ratio $E_{b,n=1}/E_{b,n=6}$ = 0.90, while $E_{b,n=1*}/E_{b,n=6}$ = 0.52. Interestingly, the corresponding ratios between the binding energy on graphene and on graphite obtained in the quantum computations mentioned above are in the range 0.8−0.9, which is consistent with the results obtained by means of the force-field of Jaffe et al. that yields θ = 100.7° on graphene (n = 1) and $\theta \approx$ 90.2° on graphite (n > 2). Furthermore, it has been suggested in experiments that only a very few layers of carbon atoms are necessary to obtain the contact angle of water on graphite.[4,5] Our study shows that the main part of the interaction between water and graphite is achieved with two layers of carbon atoms. This is in clear contrast with $E_{b,n=1*}/E_{b,n=6} \approx$ 0.52. Indeed, this value suggests that if graphite were built by stacking layers of carbon atoms that lead to θ = 127°, the first such layer would contribute to only approximately one-half of the interaction between a water molecule and graphite. In other words, both the first and second layers of carbon atoms would approximately have the same contribution to the interaction potential between water and graphite. This is in contradiction with the short-range nature of the interaction energy between a water molecule and graphene as is illustrated in Figure 4. Indeed, it can be seen that V vanishes at a distance shorter than 1 nm from the surfaces. An interpretation in terms of the work of adhesion of water can also be given. If we assume that two to three graphene layers are sufficient to establish a value of approximately 90° on graphite, a value of 127° on a graphene monolayer implies that the work of adhesion of water on this monolayer represents only 40% of the work of adhesion of water on graphite (see Table 2). This is again in contradiction with the fact that the interaction between water and graphite is mainly established through the first two carbon layers. Indeed, the fact that two layers are sufficient to establish the graphite−water interaction yields the conclusion that the work of adhesion of water on a graphene monolayer should be significantly larger than 50% of the work of adhesion of water on graphite. We conclude that the value of the contact angle for n = 1*, that is, θ = 127°, is an overestimate of the actual value. In contrast, the smooth transition in contact angle from graphite to graphene generated by the model yielding θ = 100.7° and the agreement on the ratio between binding energies obtained in quantum calculations suggest that this value of the contact angle should be considered as a more realistic experimental expectation. Assuming that the ratio between the work of adhesion on graphene and graphite is of the order of 0.82−0.85 (see Table 2), we anticipate that the contact angle of water on a graphene monolayer is of the order of 95−100°.

4. CONCLUSION

We have developed a thermodynamic model supported by MD simulations to address the unresolved question of the contact angle of water on a graphene monolayer. In particular, we have addressed the question of whether the value of 127° recently suggested in the literature is compatible with the accepted value of approximately 90−95° on graphite. We have established a connection between the change in the work of adhesion of water on both of these materials and the change in the water−surface interaction potential. We have shown that a change in θ from 90° on graphite to 127° on graphene yields a change in the work of adhesion, which is incompatible with the short-range nature of the interaction potentials between water and these carbon materials. We also have shown that the water−substrate interaction energy is the main contribution to the work of adhesion of water. However, the entropy contribution cannot be neglected to obtain a quantitative description of the work of adhesion. We interpret the work of adhesion as arising from the strength of the water−substrate interaction and from the fluctuations of this interaction. Further work is required to assess whether this interpretation is general or if it is restricted to the present systems. Finally, we anticipate that the contact angle of water on a monolayer of graphene is of the order of 95−100°. The same conclusion was very recently reached by Shih et al.[6] by means of a theory and simulations supported by experimental evidence.

AUTHOR INFORMATION

Corresponding Author

*E-mail: f.leroy@theo.chemie.tu-darmstadt.de (F.L.); vandervegt@csi.tu-darmstadt.de (N.F.A.v.d.V.).

Notes

The authors declare no competing financial interest.

■ ACKNOWLEDGMENTS

This research was supported by the German Research Foundation (DFG) within the Cluster of Excellence 259 "Smart Interfaces: Understanding and Designing Fluid Boundaries". We are grateful to the high performance computing center of the TU Darmstadt for allocating computation time and to the John von Neumann Institute for Computing in Jülich for allocating computation time on the machine JUROPA. We thank Michael Böhm and Emiliano Brini for valuable discussions. F.L. thanks Florian Müller-Plathe for his encouragement to work on the topic.

■ REFERENCES

(1) Hasan, T.; Scardaci, V.; Tan, P. H.; Bonaccorso, F.; Rozhin, A. G.; Sun, Z.; Ferrari, A. C. In *Molecular- and Nano-Tubes*; Hayden, O., Nielsch, K., Eds.; Springer Science and Business Media: New York, 2011; pp 279−354.

(2) Cohen-Tanugi, D.; Grossman, J. C. Water desalination across nanoporous graphene. *Nano Lett.* **2012**, *12*, 3602−3608.

(3) Kim, H.; Abdala, A. A.; Macosko, C. W. Graphene/polymer nanocomposites. *Macromolecules* **2010**, *43*, 6515−6530.

(4) Shin, Y. J.; Wang, Y. Y.; Huang, H.; Kalon, G.; Wee, A. T. S.; Shen, Z. X.; Bhatia, C. S.; Yang, H. Surface-energy engineering of graphene. *Langmuir* **2010**, *26*, 3798−3802.

(5) Rafiee, J.; Mi, X.; Gullapalli, H.; Thomas, A. V.; Yavari, F.; Shi, Y.; Ajayan, P. M.; Koratkar, N. A. Wetting transparency of graphene. *Nat. Mater.* **2012**, *11*, 217−222.

(6) Shih, C. J.; Wang, Q. H.; Lin, S.; Park, K. C.; Jin, Z.; Strano, M. S.; Blankschtein, D. Breakdown in the wetting transparency of graphene. *Phys. Rev. Lett.* **2012**, *109*, 176101.

(7) Wang, S. R.; Zhang, Y.; Abidi, N.; Cabrales, L. Wettability and surface free energy of graphene films. *Langmuir* **2009**, *25*, 11078−11081.

(8) Nishino, T.; Meguro, M.; Nakamae, K.; Matsushita, M.; Ueda, Y. The lowest surface free energy based on -CF3 alignment. *Langmuir* **1999**, *15*, 4321−4323.

(9) Scocchi, G.; Sergi, D.; D'Angelo, C.; Ortona, A. Wetting and contact-line effects for spherical and cylindrical droplets on graphene layers: A comparative molecular-dynamics investigation. *Phys. Rev. E* **2011**, *84*, 061602−8.

(10) Ambrosetti, A.; Silvestrelli, P. L. Adsorption of rare-gas atoms and water on graphite and graphene by van der Waals-corrected density functional theory. *J. Phys. Chem. C* **2011**, *115*, 3695−3702.

(11) Li, H.; Zeng, X. C. Wetting and interfacial properties of water nanodroplets in contact with graphene and monolayer boron-nitride sheets. *ACS Nano* **2012**, *6*, 2401−2409.

(12) Amirfazli, A.; Neumann, A. W. Status of the three-phase line tension: a review. *Adv. Colloid Interface Sci.* **2004**, *110*, 121−41.

(13) Werder, T.; Walther, J. H.; Jaffe, R. L.; Halicioglu, T.; Koumoutsakos, P. On the water-carbon interaction for use in molecular dynamics simulations of graphite and carbon nanotubes. *J. Phys. Chem. B* **2003**, *107*, 1345−1352.

(14) Weijs, J. H.; Marchand, A.; Andreotti, B.; Lohse, D.; Snoeijer, J. H. Origin of line tension for a Lennard-Jones nanodroplet. *Phys. Fluids* **2011**, *23*, 022001−11.

(15) Binder, K.; Block, B.; Das, S. K.; Virnau, P.; Winter, D. Monte Carlo methods for estimating interfacial free energies and line tensions. *J. Stat. Phys.* **2011**, *144*, 690.

(16) Ritchie, J. A.; Yazdi, J. S.; Bratko, D.; Luzar, A. Metastable sessile nanodroplets on nanopatterned surfaces. *J. Phys. Chem. C* **2012**, *116*, 8634−8641.

(17) Cao, P. X. K.; Varghese, J. O.; Heath, J. R. The microscopic structure of adsorbed water on hydrophobic surfaces under ambient conditions. *Nano Lett.* **2011**, *11*, 5581−5586.

(18) Jaffe, R. L.; Gonnet, P.; Werder, T.; Walther, J. H.; Koumoutsakos, P. Water−carbon interactions 2: Calibration of potentials using contact angle data for different interaction models. *Mol. Simul.* **2003**, *30*, 205−216.

(19) Alexiadis, A.; Kassinos, S. Molecular simulation of water in carbon nanotubes. *Chem. Rev.* **2008**, *108*, 5014−5034.

(20) Leroy, F.; Müller-Plathe, F. Interfacial excess free energies of solid-liquid interfaces by molecular dynamics simulation and thermodynamic integration. *Macromol. Rapid Commun.* **2009**, *30*, 864−70.

(21) Leroy, F.; Müller-Plathe, F. Solid-liquid surface free energy of Lennard-Jones liquid on smooth and rough surfaces computed by Molecular Dynamics using the Phantom-Wall method. *J. Chem. Phys.* **2010**, *133*, 044101−11.

(22) Weeks, J. D.; Chandler, D.; Andersen, H. C. Role of repulsive forces in forming the equilibrium structure of simple liquids. *J. Chem. Phys.* **1971**, *54*, 5237−5247.

(23) Huang, H. M.; Geissler, P. L.; Chandler, D. Scaling of hydrophobic solvation free energies. *J. Phys. Chem. B* **2001**, *105*, 6704−6709.

(24) Chandler, D. Insight review: Interfaces and the driving force of hydrophobic assembly. *Nature* **2005**, *437*, 640−647.

(25) Vega, C.; Miguel, E. d. Surface tension of the most popular models of water by using the test-area simulation method. *J. Chem. Phys.* **2007**, *126*, 154707−10.

(26) Leroy, F.; Müller-Plathe, F. Rationalization of the behavior of solid-liquid surface free energy of water in Cassie and Wenzel wetting states on rugged solid surfaces at the nanometer scale. *Langmuir* **2011**, *27*, 637−645.

(27) Berendsen, H. J. C.; Grigera, J. R.; Straatsma, T. P. The missing term in effective pair potentials. *J. Phys. Chem.* **1987**, *91*, 6269−6271.

(28) Bedrov, D.; Smith, G. D. Molecular dynamics simulation study of the structure of poly(ethylene oxide) brushes on nonpolar surfaces in aqueous solution. *Langmuir* **2006**, *22*, 6189−6194.

(29) Hess, B.; Kutzner, C.; Spoel, D. V. D.; Lindahl, E. GROMACS 4: Algorithms for highly efficient, load-balanced, and scalable molecular simulation. *J. Chem. Theory Comput.* **2008**, *4*, 435−447.

(30) Essmann, U.; Perera, L.; Berkowitz, M. L.; Darden, T.; Lee, H.; Pedersen, L. G. A smooth particle mesh Ewald method. *J. Chem. Phys.* **1995**, *103*, 8577−8593.

(31) Young, T. An essay on the cohesion of fluids. *Philos. Trans. R. Soc. London* **1805**, *95*, 65−87.

(32) Marmur, A. Soft contact: measurement and interpretation of contact angles. *Soft Matter* **2006**, *2*, 12−17.

(33) Choong, W. K. *The Determination of Contact Angle of Water on Graphite Surface: Using Grand-Canonical Transition Matrix Monte Carlo*; The State University of New York at Buffalo: New York, 2007.

(34) Machlin, E. S. On interfacial tension at a rigid apolar wall-water interface. *Langmuir* **2012**, *28*, 16729.

(35) Osborne, K. L. *Temperature-Dependence of the Contact Angle of Water on Graphite, Silicon, and Gold*; Worcester Polytechnic Institute: MA, 2009.

(36) Garcia, R.; Osborne, K.; Subashi, E. Validity of the "sharp-kink approximation" for water and other fluids. *J. Phys. Chem. B* **2008**, *112*, 8114−8119.

(37) Grzelak, E. M.; Errington, J. R. Computation of interfacial properties via Grand Canonical Transition Matrix Monte Carlo simulation. *J. Chem. Phys.* **2008**, *128*, 014710−10.

(38) Dutta, R. C.; Khan, S.; Singh, J. K. Wetting transition of water on graphite and boron-nitride surfaces: A molecular dynamics study. *Fluid Phase Equilib.* **2011**, *302*, 310−315.

(39) Ben-Naim, A. A simple model for demonstrating the relation between solubility, hydrophobic interaction, and structural changes in the solvent. *J. Phys. Chem.* **1978**, *82*, 874−885.

(40) Yu, H. A.; Karplus, M. A thermodynamic analysis of solvation. *J. Chem. Phys.* **1988**, *89*, 2366.

(41) Schravendijk, P.; van der Vegt, N. F. A. From hydrophobic to hydrophilic solvation: an application to hydration of benzene. *J. Chem. Theory Comput.* **2005**, *1*, 643−652.

(42) van der Vegt, N. F. A.; Lee, M. E.; Trzesniak, D.; Gunsteren, W. F. V. Enthalpy−entropy compensation in the effects of urea on hydrophobic interactions. *J. Phys. Chem. B* **2006**, *110*, 12852−12855.
(43) Godawat, R.; Jamadagni, S. N.; Garde, S. Characterizing hydrophobicity of interfaces using cavity formation, solute binding, and water correlations. *Proc. Natl. Acad. Sci. U.S.A.* **2009**, *106*, 15119−15124.
(44) Daoulas, K. C.; Harmandaris, V. A.; Mavrantzas, V. G. Detailed atomistic simulation of a polymer melt/solid interface: Structure, Ddensity, and conformation of a thin film of polyethylene melt adsorbed on graphite. *Macromolecules* **2008**, *38*, 5780−5795.
(45) Butt, H.-J.; Kappl, M. *Surface and Interfacial Forces*; John Wiley and Sons: New York, 2010.
(46) Gatica, S. M.; Johnson, J. K.; Zhao, X. C.; Cole, M. W. Wetting transition of water on graphite and other surfaces. *J. Phys. Chem. B* **2004**, *108*, 11704.
(47) Rubes, M. N. P.; Vondrasek, J.; Bludsky, O. Structure and stability of the water−graphite complexes. *J. Phys. Chem. C* **2009**, *113*, 8412−8419.